

Entropy Generation and Heat Transfer of Cu–Water Nanofluid Mixed Convection in a Cavity

Mliki Bouchmel, Belgacem Nabil, Abbassi Mohamed Ammar, Geudri Kamel, Omri Ahmed

Abstract—In this numerical work, mixed convection and entropy generation of Cu–water nanofluid in a lid-driven square cavity have been investigated numerically using the Lattice Boltzmann Method. Horizontal walls of the cavity are adiabatic and vertical walls have constant temperature but different values. The top wall has been considered as moving from left to right at a constant speed, U_0 . The effects of different parameters such as nanoparticle volume concentration (0–0.05), Rayleigh number (10^4 – 10^6) and Reynolds numbers (1, 10 and 100) on the entropy generation, flow and temperature fields are studied. The results have shown that addition of nanoparticles to the base fluid affects the entropy generation, flow pattern and thermal behavior especially at higher Rayleigh and low Reynolds numbers. For pure fluid as well as nanofluid, the increase of Reynolds number increases the average Nusselt number and the total entropy generation, linearly. The maximum entropy generation occurs in nanofluid at low Rayleigh number and at high Reynolds number. The minimum entropy generation occurs in pure fluid at low Rayleigh and Reynolds numbers. Also at higher Reynolds number, the effect of Cu nanoparticles on enhancement of heat transfer was decreased because the effect of lid-driven cavity was increased. The present results are validated by favorable comparisons with previously published results. The results of the problem are presented in graphical and tabular forms and discussed.

Keywords—Entropy generation, mixed convection, nanofluid, lattice Boltzmann method.

I. INTRODUCTION

OVER the past few years, the lattice Boltzmann method (LBM) has found wide-ranging applications in science and engineering [1]–[3]. This surge in interest is mainly attributed to its ability of simple and efficient computational procedure, even for complex geometries [4]–[6]. Therefore, the LBE method is able to simulate the complicated fluid flows such as multiphase flows, chemically reacting flows and visco-elastic non-Newtonian flows. The term "nanofluid" refers to a liquid containing a dispersion of submicronic solid particles (nanoparticles). The term was coined by Choi [7]. The characteristic feature of nanofluids is thermal conductivity

enhancement, a phenomenon observed by [8]. This is why intensive researches focus on the heat transfer augmentation utilizing nanofluids, and their potential in cooling industry has been carried out recently [9]–[15].

Natural convection and forced convection are two agents for convection heat transfer. To enhance heat transfer, use of mixed convection is preferred. Many numerical investigations on enhancement of buoyancy, driven by natural heat transfer using nanofluids in different geometries have been reported [16]–[19]. Lid-driven mixed convection flow is used for cooling electronic devices, lubrication purposes, drying technologies and so on. Fluid flow and heat transfer due to mixed convection driven by buoyancy and shear in a cavity filled with either pure fluid or nanofluid have been the subjects of some studies [20]–[25]. There have been few numerical investigations on entropy generation of nanofluids in cavities utilized in mixed convection.

In this study, in order to investigate entropy generation due to heat transfer and to viscous effects, similar to the geometry used by [26], a square cavity filled with Cu–water nanofluid with a moving lid at constant velocity has been considered. The effects of Reynolds number (Re) and Rayleigh number (Ra) on the fluid flow, heat transfer and entropy generation have been investigated. Simulations have been carried out for pure fluid and Cu–water nanofluid with $\phi = 5\%$ for $Ra = (10^4, 10^5 \text{ and } 10^6)$ and $Re = (1, 10 \text{ and } 100)$.

II. THE LATTICE BOLTZMANN METHOD

The LBM used here is the same as that employed in [27]–[29]. The thermal LBM utilizes two distribution functions f and g , for the flow and temperature fields respectively. It uses modelling of movement of fluid particles to capture macroscopic fluid quantities such as velocity, pressure and temperature. In this approach the fluid domain is discretized in Cartesian cells. Each cell holds a fixed number of distribution functions, which represents the number of fluid particles moving in these discrete directions. D2Q9 model for flow field, D2Q4 model for temperature field and nanoparticle concentration are used in this work. The weighting factors and the discrete particle velocity vectors are different for these two models and they are calculated with (1)–(3) as follows:

For the nine-microscopic velocities model (D2Q9) used for density distribution:

$$\omega_0 = \frac{4}{9}, \omega_i = \frac{1}{9} \text{ for } i = 1, 2, 3, 4 \text{ and } \omega_i = \frac{1}{36} \text{ for } i = 5, 6, 7, 8 \quad (1)$$

M. Bouchmel is with Unité de recherche: Matériaux, Energie et Energies Renouvelables (MEER), Faculté des Sciences de Gafsa, BP : 19, Zarroug, 2112, Gafsa, Tunisie (phone: 21626894606; e-mail: mlikibouchmel@yahoo.fr).

A. Mohamed Ammar, and O. Ahmed are with Unité de recherche: Matériaux, Energie et Energies Renouvelables (MEER), Faculté des Sciences de Gafsa, BP: 19, Zarroug, 2112, Gafsa, Tunisie (e-mail: abbassima@gmail.com, ahom206@yahoo.fr).

B. Nabil is with Unité de recherche Physique, Informatique et mathématiques faculté de sciences Gafsa, Université de Gafsa, Tunisie (e-mail: fstunis@hotmail.fr).

G. Kamel is with Mechanical Engineering Department, College of Engineering and Islamic Architecture, Umm Al-Qura University, KSA (e-mail: kamelgeudri@yahoo.fr).

$$\mathbf{c}_i = \begin{cases} 0 & i=0 \\ (\cos[(i-1)\pi/2], \sin[(i-1)\pi/2])c & i=1,2,3,4 \\ \sqrt{2}(\cos[(i-5)\pi/2+\pi/4], \sin[(i-5)\pi/2+\pi/4])c & i=5,6,7,8 \end{cases} \quad (2)$$

For the four -microscopic velocities model (D2Q4) used for internal energy distribution:

The temperature weighting factor for each direction is equal to $\omega_i' = 1/4$.

$$\mathbf{c}_i = (\cos[(i-1)\pi/2], \sin[(i-1)\pi/2])c \quad i = 1, 2, 3, 4 \quad (3)$$

The density and distribution functions i.e. the f and g , are calculated by solving the lattice Boltzmann equation (LBE), which is a special discretization of the kinetic Boltzmann equation. After introducing the BGK approximation, the general form of lattice Boltzmann equation with external force can be written as:

For the flow field:

$$f_i(\mathbf{x} + \mathbf{c}_i \Delta t, t + \Delta t) = f_i(\mathbf{x}, t) - \frac{1}{\tau_v} (f_i(\mathbf{x}, t) - f_i^{\text{eq}}(\mathbf{x}, t)) + \Delta t F_i \quad (4)$$

For the temperature field:

$$g_i(\mathbf{x} + \mathbf{c}_i \Delta t, t + \Delta t) = g_i(\mathbf{x}, t) - \frac{1}{\tau_\alpha} (g_i(\mathbf{x}, t) - g_i^{\text{eq}}(\mathbf{x}, t)) \quad (5)$$

where Δt denotes lattice time step, \mathbf{c}_i is discrete lattice velocity in direction i , F_i is the external force in direction i of lattice velocity, τ_v and τ_α are the relaxation time for the flow and temperature fields, The kinematic viscosity ν and thermal diffusivity α are respectively related to the relaxation time by (6):

$$\nu = \left[\tau_v - \frac{1}{2} \right] c_s^2 \Delta t \quad \alpha = \left[\tau_\alpha - \frac{1}{2} \right] c_s^2 \Delta t \quad (6)$$

where c_s is the lattice speed of sound which is equal to $c_s = c/\sqrt{3}$.

Furthermore, the local equilibrium distribution functions determine the type of problem that needs to be solved. They also model the equilibrium distribution functions, which are calculated with (7) and (8) for flow and temperature fields respectively.

$$f_i^{\text{eq}} = \omega_i \rho \left[1 + \frac{3(\mathbf{c}_i \cdot \mathbf{u})}{c^2} + \frac{9(\mathbf{c}_i \cdot \mathbf{u})^2}{2c^4} - \frac{3\mathbf{u}^2}{2c^2} \right] \quad (7)$$

$$g_i^{\text{eq}} = \omega_i' T \left[1 + 3 \frac{\mathbf{c}_i \cdot \mathbf{u}}{c^2} \right] \quad (8)$$

ω_i is the weighting factor for flow, ω_i' is the weighting factor for temperature and ρ is the lattice fluid density.

In order to incorporate buoyancy force in the model, the force term in (4) needs to be calculated in vertical direction (y) as:

$$F = 3\omega_i' g_y \beta \theta \quad (9)$$

For natural convection the Boussinesq approximation is applied and heat transfer is negligible. To ensure that the code works in near incompressible regime, the characteristic velocity of the flow for both natural ($V_{\text{natural}} = \sqrt{\beta g_y \Delta T H}$) and force ($V_{\text{force}} = \text{Re} \cdot \nu / H$) regimes must be small compared with the fluid speed of sound. The Reynolds number is given by:

$$\text{Re} = u_0 H / \nu \quad (10)$$

Finally, macroscopic quantities ρ , u and T can be calculated respectively by (11)-(13).

$$\rho = \sum_i f_i \quad (11)$$

$$\rho u_j = \sum_i f_i c_{ij} \quad (12)$$

$$T = \sum_i g_i \quad (13)$$

For pure fluid in the absence of nanoparticles in the enclosure, the governing equations are (4)-(13). However for modeling the nanofluid because of changing the fluid thermal conductivity, density, heat capacitance and thermal expansion, some of the governing equations should be changed.

The thermal diffusivity is written as:

$$\alpha_{nf} = \frac{k_{nf}}{(\rho c_p)_{nf}} \quad (14)$$

The effect of density at reference temperature is given by:

$$\rho_{nf} = (1 - \phi) \rho_f + \phi \rho_p \quad (15)$$

And the heat capacitance and thermal expansion of nanofluid can be given as [22]:

$$(\rho c_p)_{nf} = (1 - \phi)(\rho c_p)_f + \phi(\rho c_p)_p \quad (16)$$

$$(\rho \beta)_{nf} = (1 - \phi)(\rho \beta)_f + \phi(\rho \beta)_p \quad (17)$$

In the above equations ϕ is the solid volume fraction, ρ is the density, α is the thermal diffusivity, c_p is the specific heat at constant pressure and β is the thermal expansion coefficient.

TABLE I
THERMO PHYSICAL PROPERTIES OF FLUID AND NANOPARTICLES

Physical Properties	Fluid phase (Water)	Cu
C_p (J/kgK)	4179	385
ρ (kg/m ³)	997.1	8933
k (W/mK)	0.631	400
$\beta \times 10^{-5}$ (1/K)	21	1.6

The effective dynamic viscosity and thermal conductivity of the nanofluid as given by (18) and (19) [30]:

$$\mu_{nf} = \frac{\mu_f}{(1-\phi)^{2.5}} \quad (18)$$

$$k_{nf} = k_f \frac{k_p + 2k_f - 2\phi(k_f - k_p)}{k_p + 2k_f + \phi(k_f - k_p)} \quad (19)$$

In the convection process, the entropy generation is associated to the heat transfer and to the fluid flow friction. According to [31], the local entropy generation (s''_{gen}) can be determined by:

$$s''_{gen} = \frac{k_{nf}}{T_0^2} \left[\left(\frac{\partial T}{\partial x} \right)^2 + \left(\frac{\partial T}{\partial y} \right)^2 \right] + \frac{\mu_{nf}}{T_0} \left[2 \left(\frac{\partial u}{\partial x} \right)^2 + 2 \left(\frac{\partial v}{\partial y} \right)^2 + \left(\frac{\partial u}{\partial x} + \frac{\partial v}{\partial y} \right)^2 \right] \quad (20)$$

where $T_0 = (T_h + T_c)/2$.

The first term in (12) represents the dimensional entropy generation due to heat transfer ($s''_{gen,h}$), while the second term represents the dimensional entropy generation due to the viscous effects of the fluid ($s''_{gen,\mu}$).

III. NON-DIMENSIONAL PARAMETERS

Rayleigh number, Prandtl number and viscosity are calculated from the definition of these non-dimensional parameters [32].

$$Ra = \frac{g\beta_f H^3 (T_h - T_c)}{\nu_f \alpha_f} \quad (21)$$

$$Pr = \frac{\nu_f}{\alpha_f}, \quad \nu_f = NMac_s \sqrt{\frac{Pr}{Ra}} \quad (22)$$

Mach number should be less than $Ma = 0.3$ to insure an incompressible flow. Therefore, in the present study, Mach number was fixed at $Ma = 0.1$. The local Nusselt number, the local Sherwood number and their average values at the left walls are calculated as:

$$Nu_l = -\frac{k_{nf}}{k_f} \left(\frac{\partial \theta}{\partial X} \right)_{x=0}, \quad \overline{Nu}_l = -\frac{1}{L} \int_0^H \frac{k_{nf}}{k_f} \left(\frac{\partial \theta}{\partial X} \right)_{x=0} \quad (23)$$

IV. VALIDATION OF THE NUMERICAL CODE

Fig. 1 shows a two-dimensional square cavity with the aspect ratio equal to unity. The height of the cavity is H and its width is W . The cavity is filled either with pure water or with a suspension of copper nanoparticles in water with a volume fraction of ϕ . The left and right vertical walls are at hot and cold temperatures, respectively. The two horizontal walls are insulated and the top wall slides from left to right with uniform velocity. The thermophysical properties of nanoparticles and fluid shown in Table I are assumed constant, evaluated at the reference temperature. It is further assumed that the Boussinesq approximation is valid for buoyancy force.

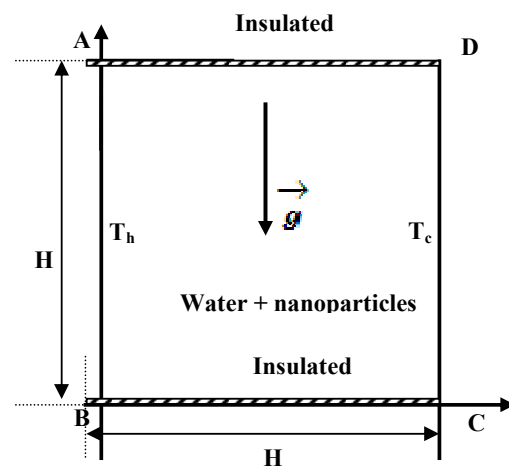


Fig. 1 Geometry and boundary conditions cavity

To validate the numerical simulation, the results for natural convection flow in an enclosed cavity filled by nanofluid have been compared with those obtained by [33]. The horizontal and vertical velocity components on the vertical and horizontal middle lines, presented in Fig. 2, show good agreement with those of [33]. In order to verify the accuracy of streamlines obtained the configuration of the cavity problem of [26] was considered. The streamlines for this cavity problem have been compared in Fig. 3 showing very good agreement. In order to validate the accuracy of entropy generation, obtained in Fig. 4 for the cavity problem of [34] at two Ra and ϕ values, we have presented the present results of contours of total entropy generation of base fluid and of Cu-Water nanofluid. Based on the aforementioned comparisons, the developed code is reliable for studying mixed convection of a nanofluid confined in a cavity.

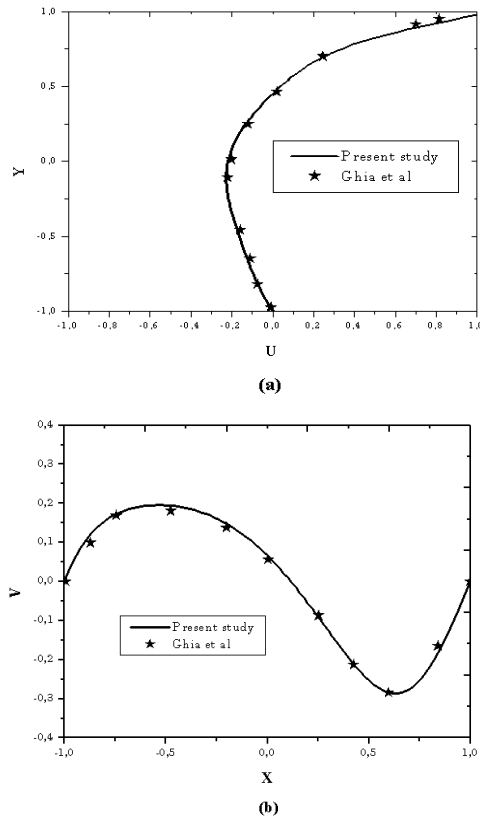


Fig. 2 (a) U velocity at $X=0.5$. (b) V velocity at $Y=0.5$ comparison with [33]

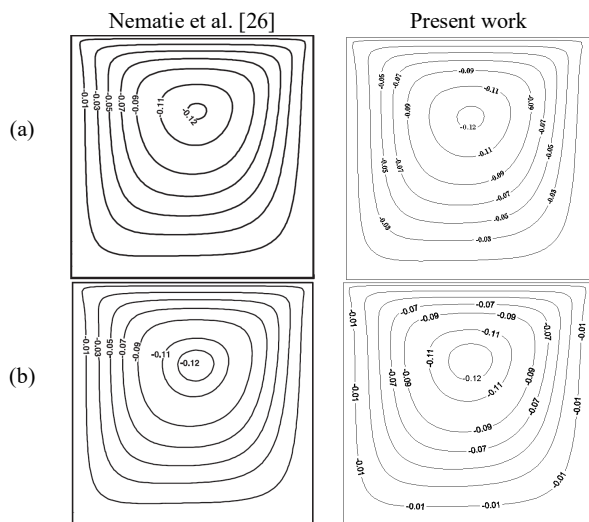


Fig. 3 Validation of Streamlines, $Ra=10^4$, $Re=10$ (a) $\phi=0.0$, (b) CuO , $\phi=0.05$

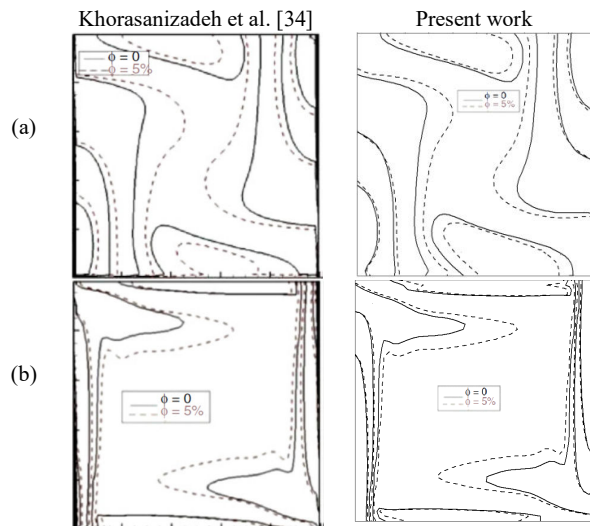


Fig. 3 Validation of Contours of total entropy generation for base fluid (solid lines) and nanofluid with $\phi=5\%$ (dashed lines) at different Ra and $Re=1$. (a) $Ra=10^4$, (b) $Ra=10^6$

V. RESULTS AND DISCUSSION

Fig. 5 demonstrates that the streamlines are mostly symmetric, showing that the effect of natural convection flow dominates lid-driven effects at $Ra=10^4$. As can be seen from Fig. 5, use of nanofluid has not changed the flow pattern but has augmented the flow intensity, so that the value of the stream function at the center of the cavity has changed from -0.8 to -1.1 . As the value of Ra increases to 10^6 , the intensity of buoyancy within the cavity increases such that the effect of lid driven flow is negligible. Also, the effect of the presence of nanoparticles on the thermal field, and temperature distribution contours, for nanofluid overlaid on that for pure fluid, the streamlines and isotherms are presented in Fig. 5 for $Re=10$, $Ra=10^5$ and 10^6 . As can be seen, use of nanofluid at Ra of 10^5 has more effect on increasing the heat penetration, because of the most effective role of the conduction heat transfer. The effect of conduction heat transfer decreases with the increase in Ra , so the nanofluid has a smaller effect on the thermal distribution.

To study the effect of the presence of nanoparticles on the streamlines, isotherms, for nanofluid and for pure fluid are presented in Fig. 6 for $Re=10$ and 100 and $Ra=10^4$. As can be seen the increase in Re augments the lid-driven forced convection flow and for $Re=100$, the effect of lid-driven flow is more dominant. In this case, the nanofluid does not have a considerable effect on the flow pattern because the buoyancy effect is insignificant.

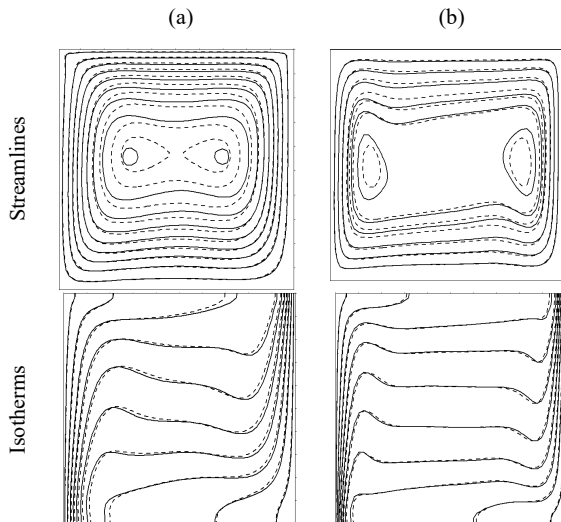


Fig. 5 Streamlines and Isotherms for base fluid (solid lines) and nanofluid with $\phi = 5\%$ (dashed lines) at $Re = 10$, (a) $Ra = 10^4$, (b) $Ra = 10^6$

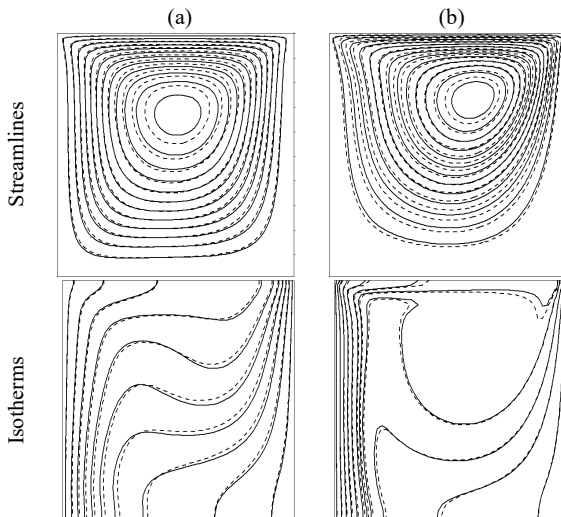


Fig. 6 Streamlines and Isotherms for base fluid (solid lines) and nanofluid with $\phi = 5\%$ (dashed lines) at $Ra = 10^4$, (a) $Re = 10$, (b) $Re = 100$

The average Nusselt number (Nu) on the left hot wall in terms of Re is shown in Fig. 7. The use of nanofluid, which increases the flow intensity, induces the rate of heat transfer, thus increases the Nu . Also increasing Re , meaning higher velocity of the top lid, increases forced convection and hence the Nu . Except for the $Ra = 10^4$, this increase seems to be not linear. Increasing Ra increases the Nu sharply for pure fluid as well as nanofluid and this increase is linear. However, use of nanofluid instead of pure fluid causes a greater increase of Nu , such that the relative increase is 52% at $Ra = 10^6$ and 28% at $Ra = 10^4$.

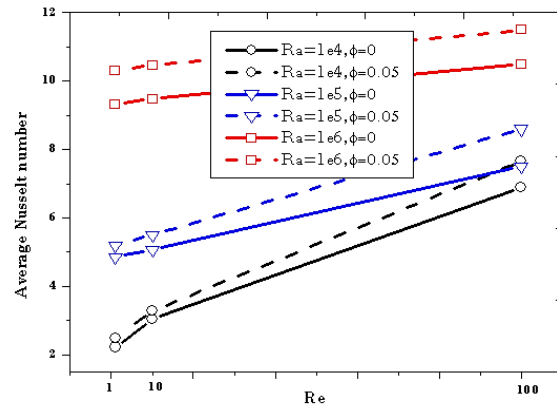


Fig. 7 Average Nusselt number on the left hot wall

Fig. 8 shows the contours of total entropy generation at $Re = 1$ and 100 for $Ra = 10^4$ and 10^6 for pure fluid as well as nanofluid. Although the symmetrical shape of contours for $Re = 1$ has remained unchanged, the total entropy generation has increased for nanofluid except in the vicinity of insulated walls. At $Re = 100$ and at $Ra = 10^4$ the symmetry does not exist anymore, but by increasing the Ra to 10^6 a change toward symmetry is somehow observed. This is the sign of the importance of effects of natural convection compared to forced convection.

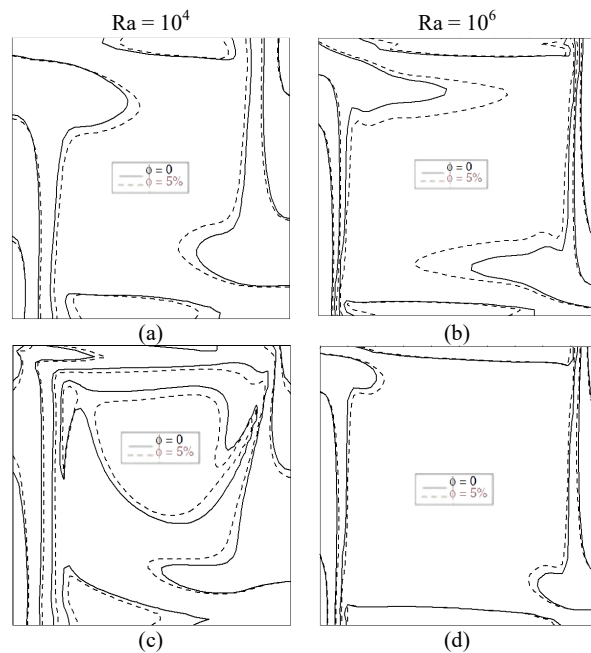


Fig. 8 Contours of total entropy generation for base fluid (solid lines) and nanofluid with $\phi = 5\%$ (dashed lines) at different Ra and Re

At $Re = 100$ and $Ra = 10^4$ from Fig. 8 (c) it is seen that, due to forced viscous effects, the intensity of contours is pronounced at the upper edge. By increasing Ra to 10^6 (Fig. 8 (d)) this intensity is also taken to the vicinity of the hot and cold walls. From Figs. 8 (a)-(c) it is seen that at the vicinity of

the walls the intensity of contours is generally pronounced such that at higher Ra numbers this intensity is observed close to the vertical walls and at higher Re numbers but low Ra numbers close to the moving top lid.

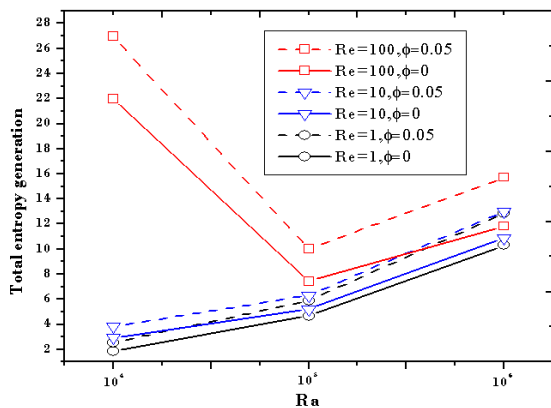


Fig. 9 Total entropy generation

VI. CONCLUSION

The lattice Boltzman method is used to investigate mixed convection of cu–water nanofluid in a cavity. The LBM results are compared with the existing conventional CFD results and a good agreement is observed. The effects of the pertinent parameters such as Rayleigh number and Reynolds number and nanoparticle volume fraction on thermal flow characteristics and on entropy generation have been investigated for a lid-driven cavity. This investigation was performed for various mentioned parameters and some conclusions were summarized as follows:

- The use of nanofluid causes a higher intensity flow and thus induces the heat transfer and produces a higher Nu.
- Increasing the values of nanoparticle volume fraction, the flow strength will be reduced in the cavity.
- Increasing the Reynolds numbers leads to a decrease in the effect of nanoparticle volume fraction because the effect of lid-driven cavity is increased.
- In general the increase of Re, Ra or use of nanofluid instead of pure fluid are resulted in higher Nu.
- Increase of the Re results, increases both terms of entropy generation.
- Except at Re = 100, the increase of Ra results, increases total entropy generation.
- The maximum and minimum entropy generations occur for nanofluid and pure fluid, respectively, use of nanofluid induces the heat transfer rate more than increasing entropy generation.
- At Ra = 10^4 , the change of Re from 1 to 100 increases Nu almost 100% and increases the total entropy generation almost 900%, while the change of Re from 1 to 10 increases Nu 23% but total entropy generation only 40%.
- At higher Ra (10^5 , 10^6) numbers, increase Re has a better effect in terms of enhanced heat transfer in comparison with increased entropy generation.

REFERENCES

- [1] M. Aghajani Delavar, M. Farhadi, K. Sedighi, "Effect of the heater location on heat transfer and entropy generation in the cavity using the lattice Boltzmann method," *Heat Trans. Res.*, vol. 40, 2009, pp. 505-519.
- [2] E. Fattahi, M. Farhadi, K. Sedighi, "Lattice Boltzmann simulation of natural convection heat transfer in eccentric annulus," *Int. J. Therm. Sci.*, vol. 49, 2010, pp. 2353-2362.
- [3] H. Huang, Z. Li, S. Liu, X.Y. Lu, "Shan-and-Chen-type multiphase lattice Boltzmann study of viscous coupling effects for two-phase flow in porous media," *Int. J. Numerical Methods Fluids*, vol. 61, 2009, pp. 341-354.
- [4] M. Mahmodi, S. M. Hashemi, "Numerical study of natural convection of a nanofluid in C-shaped enclosures," *Int. J. Thermal Sci.*, vol. 55, 2012, pp. 76-89.
- [5] M. Kalteh, H. Hasani, "Lattice Boltzmann simulation of nanofluid free convection heat transfer in an L-shaped enclosure," *Super lattices and Microstructures*, vol. 66, 2014, pp. 112-128.
- [6] H. Reza, M. Mohsen, "Magnetic field effects on natural convection flow of a nanofluid in a horizontal cylindrical annulus using Lattice Boltzmann method," *Int. J. Thermal Sci.*, vol. 64, 2013, pp. 240-250.
- [7] U.S. Choi, "Enhancing thermal conductivity of fluids with nanoparticles, developments and application of non-Newtonian flows," *ASME*, vol. 66, 1995, pp. 99-105.
- [8] K. Khanafer, K. Vafai, M. Lightstone, "Buoyancy-driven heat transfer enhancement in a two dimensional enclosure utilizing nanofluid," *Int. J. Heat Mass Transfer*, vol. 46, 2003, pp. 3639-3653.
- [9] F.H. Lai, Y.T. Yang, "Lattice Boltzmann simulation of natural convection heat transfer of Al₂O₃/water nanofluids in a square enclosure," *Int. J. Therm. Sci.*, vol. 50, 2011, pp. 1930-1941.
- [10] Z. Alloui, P. Vasseur, M. Reggio, "Natural convection of nanofluids in a shallow cavity heated from below," *Int. J. Therm. Sci.*, vol. 50, 2011, pp. 385-393.
- [11] Y. He, C. Qi, Y. Hu, B. Qin, F. Li, Y. Ding, "Lattice Boltzmann simulation of alumina–water nanofluid in a square cavity," *Nanoscale Res. Lett.*, vol. 6, 2011, pp. 1-8.
- [12] C.J. Ho, W.K. Liu, Y.S. Chang, C.C. Lin, "Natural convection heat transfer of alumina–water nanofluid in vertical square enclosures: an experimental study," *Int. J. Therm. Sci.*, vol. 49, 2010, pp. 1345-1353.
- [13] J. Rahmannedad, A. Ramezani, M. Kalteh, "Numerical investigation of magnetic field effects on mixed convection flow in a nanofluid-filled lid-driven cavity," *Int. J. Eng. Trans. A: Basics*, vol. 26, 2013, pp. 1213-1224.
- [14] A. Mahmoudi, I. Mejri, M. Ammar Abbassi, A. Omri, "Numerical Study of Natural Convection in an Inclined Triangular Cavity for Different Thermal Boundary Conditions: Application of the Lattice Boltzmann Method," *FDMP*, vol. 9, 2013, pp. 353-388.
- [15] I. Mejri, A. Mahmoudi, M. Ammar Abbassi, A. Omri, "Numerical Study of Natural Convection in an Inclined Triangular Cavity for Different Thermal Boundary Conditions: Application of the Lattice Boltzmann Method," *FDMP*, vol. 9, 2013, pp. 353-388.
- [16] G.A. Sheikhzadeh, A. Arefmanesh, M.H. Kheirkhah, R. Abdollahi, "Natural convection of Cu–water nanofluid in a cavity with partially active side walls," *Eur. J. Mech. B-Fluid*, vol. 30, 2011, pp. 166-176.
- [17] E. Abu-Nada, H.F. Oztop, "Effects of inclination angle on natural convection in enclosures filled with Cu–water nanofluid," *Int. J. Heat Fluid Fl.*, vol. 30, 2009, pp. 669-678.
- [18] S.M. Aminossadati, B. Ghasemi, "Natural convection cooling of a localised heat source at the bottom of a nanofluid-filled enclosure," *Eur. J. Mech. B-Fluid*, vol. 28, 2009, pp. 630-640.
- [19] M. Jahanshahi, S.F. Hosseini-zadeh, M. Alipanah, A. Dehghani, G.R. Vakilinejad, "Numerical simulation of free convection based on experimental measured conductivity in a square cavity using Water/SiO₂ nanofluid," *Int. Commun. Heat Mass Transfer*, vol. 37, 2010, pp. 687-694.
- [20] A. Akbarinia, A. Behzadmehr, "Numerical study of laminar mixed convection of a nanofluid in horizontal curved tubes," *Appl. Therm. Eng.*, vol. 27, 2007, pp. 1327-1337.
- [21] S. Mirmasoumi, A. Behzadmehr, "Effect of nanoparticles mean diameter on mixed convection heat transfer of a nanofluid in a horizontal tube," *Int. J. Heat Fluid Fl.*, vol. 29, 2008, pp. 557-566.
- [22] T. Basak, S. Roy, P.K. Sharma, I. Pop, "Analysis of mixed convection flows within a square cavity with uniform and non-uniform heating of bottom wall," *Int. J. Therm. Sci.*, vol. 48, 2009, pp. 891-912.

- [23] G. Guo, M.A.R. Sharif, "Mixed convection in rectangular cavities at various aspect ratios with moving isothermal sidewalls and constant flux heat source on the bottom wall," *Int. J. Therm. Sci.*, vol. 43, 2004, pp. 465–475.
- [24] R.K. Tiwari, M.K. Das, "Heat transfer augmentation in a two-sided lid-driven differentially heated square cavity utilizing nanofluids," *Int. J. Heat Mass Transfer*, vol. 50, 2007, pp. 2002–2018.
- [25] M.A. Mansour, R.A. Mohamed, M.M. Abd-Elaziz, S.E. Ahmed, "Numerical simulation of mixed convection flows in a square lid-driven cavity partially heated from below using nanofluid," *Int. Commun. Heat Mass*, vol. 37, 2010, pp. 1504–1512.
- [26] H. Nemat, M. Farhadi, K. Sedighi, E. Fattahi, A.A.R. Darzi, "Lattice Boltzmann simulation of nanofluid in lid-driven cavity," *Int. Commun. Heat Mass*, vol. 37, 2010, pp. 1528–1534.
- [27] M. Dalavar, M. Farhadi, K. Sedighi, "Numerical simulation of direct methanol fuel cells using lattice Boltzmann method," *Int. J. Hydrogen Energy*, vol. 35, 2010, pp. 9306–9317.
- [28] A. Mahmoudi, I. Mejri, M. A. Abbassi, A. Omri, "Lattice Boltzmann simulation of MHD natural convection in a Nanofluids-filled cavity with linear temperature distribution," *Powder Technology*, vol. 256, 2014, pp. 257–271.
- [29] M. Kalteh, H. Hasani, "Lattice Boltzmann simulation of nanofluid free convection heat transfer in an L-shaped enclosure," *Int. J. Superlat. Micro*, vol. 66, 2014, pp. 112–128.
- [30] Y. Xuan, Q. Li, "Heat transfer enhancement of nanofluids," *Int. J. Heat Fluid Flow*, pp. 58–64, 2000.
- [31] A. Bejan, "Entropy Generation through Heat and Fluid Flow," *Wiley, New York*, 1982.
- [32] A. Mahmoudi, I. Mejri, M. A. Abbassi, A. Omri, "Lattice Boltzmann simulation of MHD natural convection in a Nanofluids-filled cavity with linear temperature distribution," *Powder Technology*, vol. 256, 2014, pp. 257–271.
- [33] U. Ghia, K.N. Ghia, C.Y. Shin, "High-Re solutions for incompressible flow using the Navier-Stokes equations and a multigrid method," *J. Comput. Phys.*, vol. 48, 1982, pp. 387–411.
- [34] H. Khorasanizadeh, M. Nikfar, J. Amani, "Entropy generation of Cu–water nanofluid mixed convection in a cavity," *Eur. J. Mech. B. Fluids*, vol. 37, 2013, pp. 143–152.